GEOPHYSICS, VOL. 73, NO. 5 (SEPTEMBER-OCTOBER 2008); P. VE205–VE210, 5 FIGS.
10.1190/1.2967501

Time-to-depth conversion and seismic velocity estimation using time-migration velocity

Maria Cameron[1], Sergey Fomel[2], and James Sethian[3]

ABSTRACT

The objective was to build an efficient algorithm (1) to estimate seismic velocity from time-migration velocity, and (2) to convert time-migrated images to depth. We established theoretical relations between the time-migration velocity and seismic velocity in two and three dimensions using paraxial ray-tracing theory. The relation in two dimensions implies that the conventional Dix velocity is the ratio of the interval seismic velocity and the geometric spreading of image rays. We formulated an inverse problem of finding seismic velocity from the Dix velocity and developed a numerical procedure for solving it. The procedure consists of two steps: (1) computation of the geometric spreading of image rays and the true seismic velocity in time-domain coordinates from the Dix velocity; (2) conversion of the true seismic velocity from the time domain to the depth domain and computation of the transition matrices from time-domain coordinates to depth. For step 1, we derived a partial differential equation (PDE) in two and three dimensions relating the Dix velocity and the geometric spreading of image rays to be found. This is a nonlinear elliptic PDE. The physical setting allows us to pose a Cauchy problem for it. This problem is ill posed, but we can solve it numerically in two ways on the required interval of time, if it is sufficiently short. One way is a finite-difference scheme inspired by the Lax-Friedrichs method. The second way is a spectral Chebyshev method. For step 2, we developed an efficient Dijkstra-like solver motivated by Sethian's fast marching method. We tested numerical procedures on a synthetic data example and applied them to a field data example. We demonstrated that the algorithms produce a significantly more accurate estimate of seismic velocity than the conventional Dix inversion. This velocity estimate can be used as a reasonable first guess in building velocity models for depth imaging.

INTRODUCTION

Time-domain seismic imaging is a robust and efficient process routinely applied to seismic data (Yilmaz, 2001; Robein, 2003). Rapid scanning and determination of time-migration velocity can be accomplished either by repeated migrations (Yilmaz et al., 2001) or by velocity continuation (Fomel, 2003). Time migration is considered adequate for seismic imaging in areas with mild lateral velocity variations. However, even mild variations can cause structural distortions of time-migrated images and render them inadequate for accurate geologic interpretation of subsurface structures.

To remove structural errors inherent in time migration, it is necessary to convert time-migrated images into the depth domain, either by migrating the original data with a prestack depth-migration algorithm or by depth migrating poststack data after time demigration (Kim et al., 1997). Each option requires converting the time-migration velocity to a velocity model in depth.

The connection between the time- and depth-domain coordinates is provided by the concept of image ray, which was introduced by Hubral (1977). Image rays are seismic rays that arrive normal to the earth's surface. Hubral's theory explains how a depth velocity model can be converted to time coordinates. However, it does not explain how a depth velocity model can be converted to the time-migration velocity.

Moreover, image-ray tracing is a numerically inconvenient procedure for achieving uniform coverage of the subsurface. This could explain why simplified image-ray-tracing algorithms (Larner et al., 1981; Hatton et al., 1981) did not find widespread practical applica-

Manuscript received by the Editor 22 May 2008; published online 1 October 2008.
[1]New York University, Department of Mathematics, Courant Institute of Mathematical Science, New York, New York, U.S.A. E-mail: kourkina@earthlink.net.
[2]The University of Texas at Austin, Bureau of Economic Geology, John A. and Katherine G. Jackson School of Geosciences, Austin, Texas, U.S.A. E-mail: sergey.fomel@beg.utexas.edu.
[3]University of California at Berkeley, Department of Mathematics, Berkeley, California, U.S.A. E-mail: sethian@math.berkeley.edu.

tions. Other limitations of image rays are related to the inability of time migration to handle large lateral variations in velocity (Bevc et al., 1995; Robein, 2003).

The objective of this work is to find an efficient method for building a velocity model from time-migration velocity. We establish new ray-theoretical connections between time-migration velocity and seismic velocity in two and three dimensions. These results are based on the image-ray theory and paraxial ray-tracing theory (Popov and Pšenčik, 1978; Červený, 2001; Popov, 2002).

The results can be viewed as an extension of the Dix formula (Dix, 1955) to laterally inhomogeneous media. We show that the Dix velocity is seismic velocity divided by the geometric spreading of image rays. Hence, we use the Dix velocity instead of time-migration velocity as a more convenient input. We develop a numerical approach to find (1) seismic velocity from the Dix velocity, and (2) transition matrices from time-domain coordinates to depth-domain coordinates. We test the approach on synthetic and field data examples. This approach is complementary to more traditional velocity-estimation methods. It can be used as the first step in a velocity model-building process.

TIME-MIGRATION VELOCITY

Kirchhoff prestack time migration commonly is based on the following traveltime approximation (Yilmaz, 2001). Let **s** be a source, **r** be a receiver, and **x** be the reflection subsurface point. Then the total traveltime from **s** to **x** and from **x** to **r** is approximated as

$$T(\mathbf{s},\mathbf{x}) + T(\mathbf{x},\mathbf{r}) \approx \hat{T}(\mathbf{x}_0,t_0,\mathbf{s},\mathbf{r}), \tag{1}$$

where $\mathbf{x}_0$ and t_0 are effective parameters of the subsurface point **x**.

The approximation $\hat{T}$ usually takes the form of the double-square-root equation

$$\hat{T}(\mathbf{x}_0,t_0,\mathbf{s},\mathbf{r}) = \sqrt{t_0^2 + \frac{|\mathbf{x}_0-\mathbf{s}|^2}{V_m^2(\mathbf{x}_0,t_0)}} + \sqrt{t_0^2 + \frac{|\mathbf{x}_0-\mathbf{r}|^2}{V_m^2(\mathbf{x}_0,t_0)}}, \tag{2}$$

where $\mathbf{x}_0$ and t_0 are the escape location and traveltime of the image ray (Hubral, 1977) from the subsurface point **x**. Regarding this approximation, let us list four cases depending on the seismic velocity V and the dimension of the problem:

1) Velocity V is constant. Equation 2 is exact, and $V_m = V$.
2) Velocity V depends on only the depth z. Equation 2 is a consequence of the truncated Taylor expansion for the traveltime around the surface point $\mathbf{x}_0$. Velocity V_m depends on only t_0 and is the root-mean-square velocity

$$V_m(t_0) = \sqrt{\frac{1}{t_0}\int_0^{t_0} V^2(z(t))dt}. \tag{3}$$

In this case, the Dix inversion formula (Dix, 1955) is exact. We formally define the Dix velocity $V_{\mathrm{Dix}}(t)$ by inverting equation 3 as follows:

$$V_{\mathrm{Dix}}(t_0) = \sqrt{\frac{d}{dt_0}(t_0 V_m^2(t_0))}. \tag{4}$$

3) Velocity is arbitrary in two dimensions. Equation 2 is a consequence of the truncated Taylor expansion for the traveltime around the surface point x_0. Velocity $V_m(x_0,t_0)$ is a certain kind of mean velocity, and we establish its exact meaning in the next section.
4) Velocity is arbitrary in three dimensions. Equation 2 is heuristic and not a consequence of the truncated Taylor expansion. To write an analog of traveltime approximation 2 for the three-dimensional case, we use the relation (Hubral and Krey, 1980)

$$\mathbf{\Gamma} = [V(\mathbf{x}_0)\mathbf{R}(\mathbf{x}_0,t_0)]^{-1}, \tag{5}$$

where $\mathbf{\Gamma}$ is the matrix of the second derivatives of the traveltimes from a subsurface point **x** to the surface, **R** is the matrix of radii of curvature of the emerging wavefront from the point source **x**, and $V(\mathbf{x}_0)$ is the velocity at the surface point $\mathbf{x}_0$.

For convenience, we prefer to deal with matrix $\mathbf{K} \equiv \mathbf{\Gamma}^{-1}$, which is, according to equation 5,

$$\mathbf{K}(\mathbf{x}_0,t_0) \equiv V(\mathbf{x}_0)\mathbf{R}(\mathbf{x}_0,t_0). \tag{6}$$

The traveltime approximation for three dimensions implied by the Taylor expansion is

$$\hat{T}(\mathbf{x}_0,t_0,\mathbf{s},\mathbf{r}) = \sqrt{t_0^2 + t_0(\mathbf{x}_0-\mathbf{s})^T[\mathbf{K}(\mathbf{x}_0,t_0)]^{-1}(\mathbf{x}_0-\mathbf{s})} + \sqrt{t_0^2 + t_0(\mathbf{x}_0-\mathbf{r})^T[\mathbf{K}(\mathbf{x}_0,t_0)]^{-1}(\mathbf{x}_0-\mathbf{r})}. \tag{7}$$

The entries of the matrix $\mathbf{K}(\mathbf{x}_0,t_0)$ have dimensions of squared velocity and can be chosen optimally in the process of time migration.

It is possible to show, however, that one needs only the values of

$$\det\left(\frac{\partial}{\partial t_0}\mathbf{K}(\mathbf{x}_0,t_0)\right) \tag{8}$$

to perform the inversion. This means that the conventional 3D prestack time migration with traveltime approximation 2 provides sufficient input for the inversion procedure in the 3D case. The determinant in equation 8 is well approximated by the square of the Dix velocity obtained from the 3D prestack time migration using the approximation given by equation 2.

One can use more complex and accurate approximations than the double-square-root equations 2 and 7, e.g., the shifted hyperbola approximation (Siliqi and Bousquié, 2000). However, other known approximations also involve parameters equivalent to V_m or **K**.

SEISMIC VELOCITY

In this section, we establish theoretical relationships between time-migration velocity and seismic velocity in two and three dimensions.

The seismic velocity and Dix velocity are connected through the quantity $|\mathbf{Q}|$, the geometric spreading of image rays. The quantity $|\mathbf{Q}|$ is a scalar in two dimensions and a 2×2 matrix in three dimensions. The simplest way to introduce **Q** is the following. Trace an image ray $\mathbf{x}(\mathbf{x}_0,t)$; $\mathbf{x}_0$ is the starting surface point, and t is the traveltime. Call this ray central. Consider a small tube of rays around it. All these

rays start from a small neighborhood $d\mathbf{x}_0$ of the point $\mathbf{x}_0$ perpendicular to the earth's surface. Thus, they represent a fragment of a plane wave propagating downward.

Consider a fragment of the wavefront defined by this ray tube at time t_0. Let $d\mathbf{q}$ be the fragment of the tangent to the front at the point $\mathbf{x}(\mathbf{x}_0,t_0)$ reached by the central ray at time t_0 and bounded by the ray tube (Figure 1). Then, in two dimensions, Q is the derivative $Q(x_0,t_0) = dq/dx_0$. In three dimensions, $\mathbf{Q}$ is the matrix of the derivatives $\mathbf{Q}_{ij}(\mathbf{x}_0,t_0) = d\mathbf{q}_i/d\mathbf{x}_{0j}$, $i,j = 1,2$, where derivatives are taken along certain mutually orthogonal directions $\mathbf{e}_1$, $\mathbf{e}_2$ (Popov and Pšenčik, 1978; Červený, 2001; Popov, 2002).

The time evolution of the matrices $\mathbf{Q}$ and $\mathbf{P}$ is given by

$$\frac{d}{dt}\begin{pmatrix}\mathbf{Q}\\ \mathbf{P}\end{pmatrix} = \begin{pmatrix} 0 & V_0^2\mathbf{I}\\ -\dfrac{1}{V_0}\mathbf{V} & 0\end{pmatrix}\begin{pmatrix}\mathbf{Q}\\ \mathbf{P}\end{pmatrix}, \tag{9}$$

where V_0 it the velocity at the central ray at time t, $\mathbf{V} = (\partial^2 V/\partial q_i \partial q_j)_{i,j=1,2}$, and $\mathbf{I}$ is the 2×2 identity matrix. The absolute value of det $\mathbf{Q}$ has a simple meaning: it is the geometric spreading of image rays (Popov and Pšenčik, 1978; Červený, 2001; Popov, 2002). The matrix $\mathbf{\Gamma}$, introduced in the previous section, relates to $\mathbf{Q}$ and $\mathbf{P}$ as $\mathbf{\Gamma} = \mathbf{P}\mathbf{Q}^{-1}$. Hence, $\mathbf{K} = \mathbf{Q}\mathbf{P}^{-1}$.

In Cameron et al. (2007), we prove that

$$V_{\mathrm{Dix}}(x_0,t_0) \equiv \sqrt{\frac{\partial}{\partial t_0}(t_0 V_m^2(x_0,t_0))} = \frac{V(x(x_0,t_0),z(x_0,t_0))}{|Q(x_0,t_0)|} \tag{10}$$

in two dimensions, where $V_m(x_0,t_0)$ is the time-migration velocity; and

$$\frac{\partial}{\partial t_0}(\mathbf{K}(\mathbf{x}_0,t_0)) = V(\mathbf{x}(\mathbf{x}_0,t_0))(\mathbf{Q}(\mathbf{x}_0,t_0)\mathbf{Q}^T(\mathbf{x}_0,t_0))^{-1} \tag{11}$$

in three dimensions, where $\mathbf{K}$ is defined by equation 6 and can be determined from equation 7.

PARTIAL DIFFERENTIAL EQUATIONS FOR THE GEOMETRIC SPREADING OF IMAGE RAYS

In this section, we derive the partial differential equations for Q in two and three dimensions. From now on, we denote the square of the Dix velocity by f in two dimensions and the corresponding matrix by $\mathbf{F}$ in three dimensions, to avoid the subscript

$$\mathbf{F} \equiv \frac{\partial}{\partial t_0}(\mathbf{K}(\mathbf{x}_0,t_0)). \tag{12}$$

Furthermore, we imply that t_0 denotes the one-way traveltime along the image rays. Finally, we assume that the domain does not contain caustics; i.e., the image rays do not cross on the interval of time we consider.

2D case

Consider a set of image rays coming to the surface. Suppose we are tracing them all backward in time along with the quantities Q and P. Let us eliminate the unknown velocity V in system 9 using equation 10. Moreover, let us eliminate the differentiation in q using the definition of Q and rewrite it in the time-domain coordinates x_0,t_0. Indeed, $Q = dq/dx_0$, hence $d/dq = (dx_0/dq)(d/dx_0) = Q^{-1}d/dx_0$. Therefore, system 9 becomes

$$Q_{t_0} = (fQ)^2 P, \quad P_{t_0} = -\frac{1}{fQ}\left(\frac{(fQ)_{x_0}}{Q}\right)_{x_0}. \tag{13}$$

Eliminating P in system 13, we get the following partial differential equation (PDE) for Q,

$$\left(\frac{Q_{t_0}}{f^2Q^2}\right)_{t_0} = -\frac{1}{fQ}\left(\frac{(fQ)_{x_0}}{Q}\right)_{x_0}. \tag{14}$$

The initial conditions are $Q(x_0,0) = 1$, $Q_{t_0}(x_0,0) = 0$. Equation 14 simplifies in terms of the negative reciprocal of Q as follows. Introduce $y = -1/Q$. Then equation 14 becomes

$$\left(\frac{y_{t_0}}{f^2}\right)_{t_0} = \frac{y}{f}\left(\left(\frac{f}{y}\right)_{x_0} y\right)_{x_0}. \tag{15}$$

In the expanded form, equation 15 is

$$\frac{y_{t_0t_0}}{f^2} - 2\frac{y_{t_0}f_{t_0}}{f^3} = y\frac{f_{x_0x_0}}{f} - y_{x_0}\frac{f_{x_0}}{f} - y_{x_0x_0} + \frac{y_{x_0}^2}{y}. \tag{16}$$

3D case

Equation 11 can be rewritten in the following form,

$$V = \sqrt[4]{\det \mathbf{F}(\det \mathbf{Q})^2}, \tag{17}$$

where $\mathbf{F}$ is the left-hand side of equation 11. As in the 2D case, we rewrite system 9 in time-domain coordinates $(\mathbf{x}_0,t_0)$. Then we get

$$\mathbf{Q}_{t_0} = V^2\mathbf{P}, \tag{18}$$

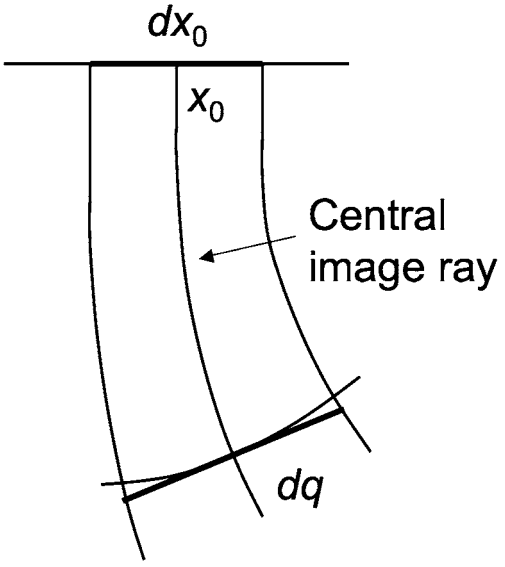

Figure 1. Illustration for the definition of geometric spreading.

$$\mathbf{P}_{t_0} = -\frac{1}{V}\mathbf{Q}^{-1}[\nabla(\mathbf{Q}^{-1}\nabla V)^T]\mathbf{Q}, \quad (19)$$

where V is given by equation 17, and the gradients are taken with respect to $\mathbf{x}_0$.

Then the PDE for $\mathbf{Q}$ is

$$\left(\frac{1}{V^2}\mathbf{Q}_{t_0}\right)_{t_0} = -\frac{1}{V}\mathbf{Q}^{-1}[\nabla(\mathbf{Q}^{-1}\nabla V)^T]\mathbf{Q}. \quad (20)$$

The initial conditions are $\mathbf{Q}(\mathbf{x}_0,0) = \mathbf{I}_2, \mathbf{Q}_{t_0}(\mathbf{x}_0,0) = 0$. The required input $\sqrt{\det \mathbf{F}}$ is well approximated by the squares of the Dix velocity obtained from the 3D prestack time migration. We emphasize that despite the fact that $\mathbf{Q}$ is a matrix in three dimensions, scalar data are enough for its computation.

Cauchy problem for elliptical equations

Equations 14 and 20 reveal the nature of the instabilities in the problem at hand. These PDEs are elliptic. The physical setting allows us to pose only a Cauchy problem for them, which is known to be ill-posed. Furthermore, the PDEs involve not only the Dix velocity, but also its first and second derivatives. This dependency leads to high sensitivity of the solutions to input data.

Nonetheless, we found two ways for solving these PDEs numerically on the required, and relatively short, interval of time: namely, a finite-difference scheme inspired by the Lax-Friedrichs method and a spectral Chebyshev method. A detailed analysis of the problem shows that these methods work because of

1) the special input V_{Dix}, corresponding to a positive finite seismic velocity
2) the special initial conditions $Q(x_0,t_0 = 0) = 1$, $Q_t(x_0,t_0 = 0) = 0$ that correspond to the image rays
3) the fact that our methods damp the high harmonics (either by including error terms in the finite-difference method or by truncation of the polynomial series in the spectral Chebyshev method)
4) the short interval of time, in which we need to compute the solution so that the growing low harmonics fail to develop significantly

Items 1 and 2 say that the exact solutions of PDEs for the hypothetical, perfect Dix velocity given by equations 10 and 11 are finite and nonzero. Items 3 and 4 say that the numerical methods take care of the imperfection of the data and computations on a short-enough time interval.

INVERSION METHODS

Numerical reconstruction of true seismic velocity $V(\mathbf{x})$ in depth-domain coordinates from the Dix velocity given in the time-domain coordinates $(\mathbf{x}_0,t_0)$ consists of two steps:

Step 1. Compute the geometric spreading of image rays in the time-domain coordinates from the Dix velocity by solving equation 14 in two dimensions and equation 20 in three dimensions. Then find $V(\mathbf{x}_0,t_0)$ from equation 10 in two dimensions and equation 17 in three dimensions.

Step 2. Convert the seismic velocity $V(\mathbf{x}_0,t_0)$ in the time-domain coordinates to depth-domain coordinates $\mathbf{x}$ using the time-to-depth conversion algorithm, which is presented by Cameron et al. (2007). It is a fast and robust Dijkstra-like solver motivated by the Fast Marching Method (Sethian, 1996, 1999).

We performed step 1 in two ways, a finite difference method and a spectral Chebyshev method.

Finite-difference method

This method was inspired by the Lax-Friedrichs method for hyperbolic conservation laws (Lax, 1954) because of its total variation diminishing property. We use the "Lax-Friedrichs averaging" and wide five-point stencil in space. The scheme is given by

$$P_j^{n+1} = \frac{P_{j+1}^n + P_{j-1}^n}{2} - \frac{\Delta t}{4\Delta x}\frac{1}{V_j^n} \times\left(\frac{V_{j+2}^n - V_j^n}{Q_{j+1}^n} - \frac{V_j^n - V_{j-2}^n}{Q_{j-1}^n}\right), \quad (21)$$

$$-\frac{1}{Q_j^{n+1}} = -\frac{1}{Q_j^n} + \frac{\Delta t}{2}((f_j^n)^2 P_j^n + (f_j^{n+1})^2 P_j^{n+1}), \quad (22)$$

where $V \equiv fQ$.

We impose the following boundary conditions $Q_0^n = Q_{nx-1}^n = 1$, $P_0^n = P_{nx-1}^n = 0$ corresponding to the straight boundary rays. We set the initial conditions $Q_j^0 = 1$, $P_j^0 = 0$ corresponding to the initial conditions for the image rays traced backward: $Q = 1, P = 0$.

Spectral Chebyshev method

Alternatively, we solve the PDE in the form given by equation 15 by a spectral Chebyshev method (Boyd, 2001). Using cubic splines, we define the input data at N_{coef} Chebyshev points. We compute the Chebyshev coefficients and coefficients of the derivatives in the right-hand side of equation 15. Then we use a smaller number N_{eval} of the coefficients for function evaluation. We need to do such Chebyshev differentiation twice.

Finally, we perform the time step using the stable third-order Adams-Bashforth method (Boyd, 2001), which is

$$u^{n+1} = u^n + \Delta t\left(\frac{23}{12}F^n - \frac{4}{3}F^{n-1} + \frac{5}{12}F^{n-2}\right), \quad (23)$$

where $F^n \equiv F(u^n,x,t^n)$ is the right-hand side. In numerical examples, we tried $N_{\text{coef}} \geq 100$ and $N_{\text{eval}} \leq 25$. This method allows larger time steps than the finite-difference method, and it has the adjustable parameter N_{eval}.

For step 2, we use a Dijkstra-like solver introduced in Cameron et al. (2007). It is an efficient time-to-depth conversion algorithm motivated by the fast marching method (Sethian, 1996). The input for this algorithm is $V(x_0,t_0)$, and the outputs are the seismic velocity $V(x,z)$ and the transition matrices from time-domain to depth-domain coordinates $x_0(x,z)$ and $t_0(x,z)$.

We solve the eikonal equation with an unknown right-hand side coupled with the orthogonality relation

$$|\nabla t_0| = \frac{1}{V(x_0(x,z),t_0(x,z))}, \quad \nabla t_0 \cdot \nabla x_0 = 0. \quad (24)$$

The orthogonality relation means that the image rays are orthogonal to the wavefronts. Such time-to-depth conversion is very fast and produces the outputs directly on the depth-domain grid.

EXAMPLES

Synthetic data example

Figure 2a shows a synthetic velocity model. The model contains a high-velocity anomaly that is asymmetric and decays exponentially. The corresponding Dix velocity mapped from time to depth is shown in Figure 2b. There is a significant difference between both the value and shape of the velocity anomaly recovered by the Dix method and the true anomaly. The difference is explained by taking into account geometric spreading of image rays. Figure 2c shows the velocity recovered by our method and the corresponding family of image rays. An analogous 3D example is provided in Cameron et al. (2007).

Field data example

Figure 3, taken from Fomel (2003), shows a prestack time-migrated image from the North Sea and corresponding time-migration velocity obtained by velocity continuation. The most prominent feature in the image is a salt body, which causes significant lateral variations of velocity.

Figure 4 compares the Dix velocity converted to depth with the interval velocity model recovered by our method. As in the synthetic example, there is a significant difference between the two velocities caused by the geometric spreading of image rays. The middle part of the velocity model might not be recovered properly. The true structure should include a salt body visible in the image. The inability of our method to recover it exactly shows the limitation of the proposed approach in the areas of significant lateral velocity variations, which invalidate the assumptions behind time migration (Robein, 2003).

Figure 5 compares three images: poststack depth-migration image using Dix velocity, poststack depth-migration image using the velocity estimated by our method, and prestack time-migration image converted to depth with our algorithm. The evident structural improvements in Figure 5b in comparison with Figure 5a, in particular near salt flanks, and a good structural agreement between Figure 5b and c, serve as an indirect evidence of the algorithm's success. An ultimate validation should come from prestack depth-migration velocity analysis, which is significantly more expensive.

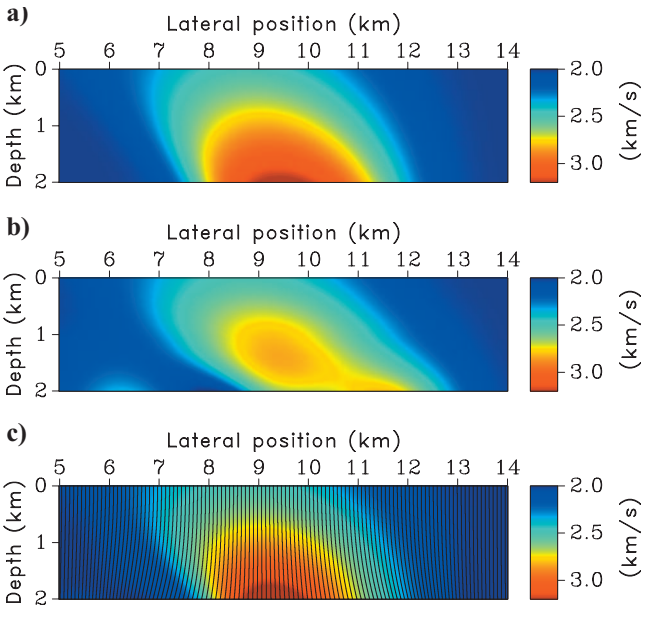

Figure 2. Synthetic test on interval velocity estimation. (a) Exact velocity model. (b) Dix velocity converted to depth. (c) Estimated velocity model and the corresponding image rays. The image-ray spreading causes significant differences between Dix velocity and estimated velocity.

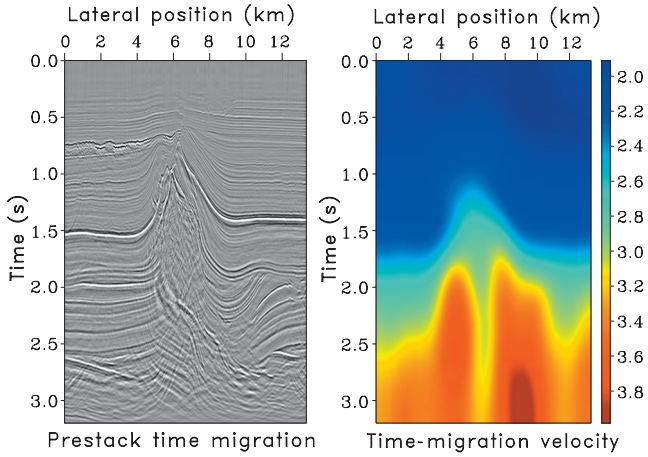

Figure 3. (a) Seismic image from the North Sea obtained by prestack time migration using velocity continuation (Fomel, 2003). (b) Corresponding time-migration velocity.

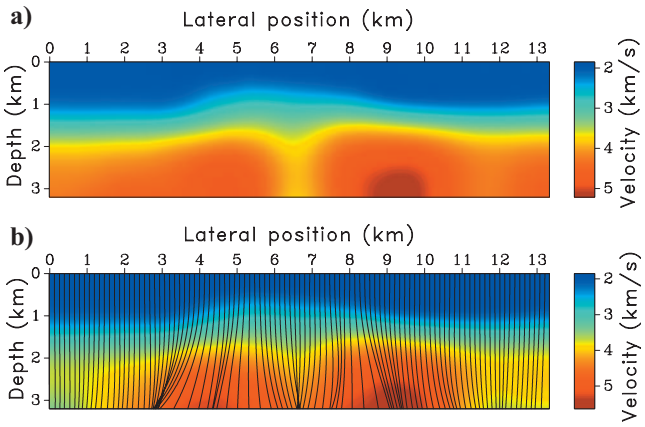

Figure 4. Field data example of interval velocity estimation. (a) Dix velocity converted to depth. (b) Estimated velocity model and the corresponding image rays. The image-ray spreading causes significant differences between Dix velocity and true velocity.

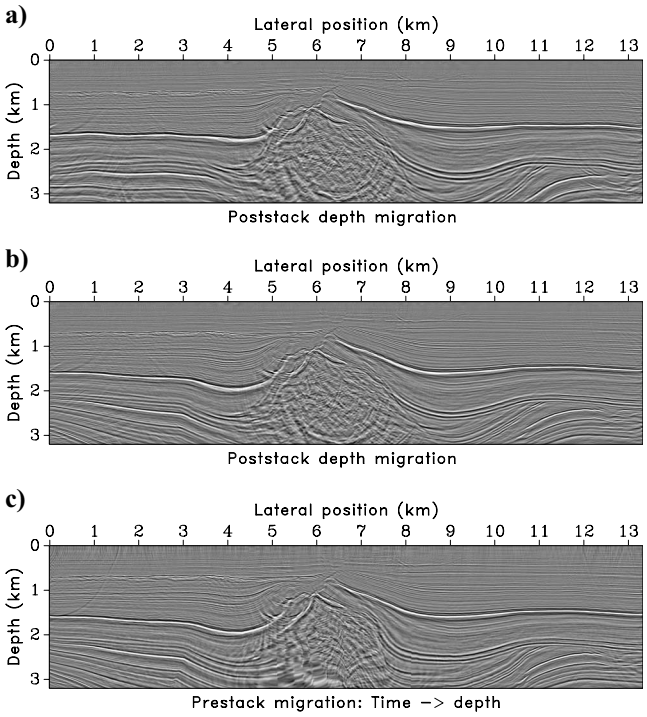

Figure 5. Migrated images of the field data example. (a) Poststack migration using Dix velocity. (b) Poststack migration using estimated velocity. (c) Prestack time migration converted to depth with our algorithm.

CONCLUSIONS

We have applied the recently established theorem that the Dix velocity obtainable from time-migration velocity is the true interval velocity divided by the geometric spreading of image rays to pose the corresponding inverse problem.

We have suggested a set of numerical algorithms for solving the problem numerically. We have tested these algorithms on a synthetic data example with laterally heterogeneous velocity and demonstrated that they produce significantly better results than simple Dix inversion followed by time-to-depth conversion. Moreover, the Dix velocity might differ qualitatively from the output velocity. We have also tested our algorithm on a field data example and validated it by comparing a prestack time-migration image mapped to depth with poststack depth migrated images.

Our approach is complementary to velocity estimation methods that work directly in the depth domain. Therefore, it can serve as an efficient first step in seismic velocity model building.

REFERENCES

Bevc, D., J. L. Black, and G. Palacharla, 1995, Plumes: Response of time migration to lateral velocity variation: Geophysics, **60**, 1118–1127.

Boyd, J. P., 2001, Chebyshev and Fourier spectral methods, 2nd ed.: Dover Publications.

Cameron, M., S. Fomel, and J. Sethian, 2007, Seismic velocity estimation from time migration: Inverse Problems, **23**, 1329–1369.

Červený, V., 2001, Seismic ray method: Cambridge University Press.

Dix, C. H., 1955, Seismic velocities from surface measurements: Geophysics, **20**, 68–86.

Fomel, S., 2003, Time-migration velocity analysis by velocity continuation: Geophysics, **68**, 1662–1672.

Hatton, L., K. L. Larner, and B. S. Gibson, 1981, Migration of seismic data from inhomogeneous media: Geophysics, **46**, 751–767.

Hubral, P., 1977, Time migration—Some ray theoretical aspects: Geophysical Prospecting, **25**, 738–745.

Hubral, P., and T. Krey, 1980, Interval velocities from seismic reflection time measurements: SEG.

Kim, Y. C., W. B. Hurt, L. J. Maher, and P. J. Starich, 1997, Hybrid migration: A cost-effective 3-D depth-imaging technique: Geophysics, **62**, 568–576.

Larner, K. L., L. Hatton, B. S. Gibson, and I. S. Hsu, 1981, Depth migration of imaged time sections: Geophysics, **46**, 734–750.

Lax, P. D., 1954, Weak solutions of hyperbolic equations and their numerical computation: Communications in Pure and Applied Mathematics, **7**, 159–193.

Popov, M. M., 2002, Ray theory and Gaussian beam method for geophysicists: Editora da Universidade Federal da Bahia.

Popov, M. M., and I. Pšenčik, 1978, Computation of ray amplitudes in inhomogeneous media with curved interfaces: Studia Geophysica et Geodaetica, **22**, 248–258.

Robein, E., 2003, Velocities, time-imaging and depth-imaging in reflection seismics: EAGE.

Sethian, J., 1996, Fast marching level set method for monotonically advancing fronts: Proceedings of the National Academy of Sciences, 93, 1591–1595.

——–, 1999, Fast marching methods: SIAM Review, **41**, 199–235.

Siliqi, R., and N. Bousquié, 2000, Anelliptic time processing based on a shifted hyperbola approach: 70th Annual International Meeting, SEG, Expanded Abstracts, 2245–2248.

Yilmaz, O., 2001, Seismic data analysis: SEG.

Yilmaz, O., I. Tanir, and C. Gregory, 2001, A unified 3-D seismic workflow: Geophysics, **66**, 1699–1713.